

C80-003

Flight Effects on Noise Generated by a JT8D Engine with Inverted Primary/Fan Flow

00023

Frank G. Strout*

Boeing Commercial Airplane Company, Seattle, Wash.

and

Adolph Atencio Jr.†

NASA Ames Directorate, Moffett Field, Calif.

A JT8D-17R engine with inverted primary and fan flows was tested under static conditions and in the NASA-Ames 40×80 ft wind tunnel to determine static and flight noise characteristics. The major purpose of the program was to evaluate flight effects on noise generated by the inverted flow profile of a large-scale engine. This jet noise suppressor concept is of particular interest to advanced supersonic transport engine cycle studies where high jet velocities create a serious noise problem during takeoff operation. The engine with inverted flow was tested with conical, plug, 20-lobe nozzles, and an acoustic shield. Wind-tunnel results show that forward velocity causes a significant reduction in peak PNL suppression, but only modest reductions in peak OASPL and EPNL suppression. The flight EPNL suppression ranged from 4.0 EPNdB for the basic inverter to 7.5 EPNdB for the inverter with 20-lobe nozzle and acoustic shield. When compared with the JT8D engine with internal mixer, the inverted flow configuration provides comparable EPNL suppression under flight conditions.

Introduction

STATIC model tests conducted by Boeing and others in industry have shown that inverting the primary and fan streams of a turbofan engine offers significant potential for reducing jet noise. The suppression concept is of particular interest to Advanced Supersonic Transport (AST) engine cycle studies where high jet velocities create a serious noise problem during takeoff operations. Although NASA is sponsoring programs to determine static and simulated flight suppression characteristics of model jets with inverted flow, the influence of scaling and engine operating characteristics on the effectiveness of the inverted flow concept will remain as a major concern.

NASA ARC contract NAS2-9302 was conducted to establish the static and flight noise characteristics of a JT8D engine with inverted primary and fan flow.¹ The JT8D engine matched important AST cycle flow parameters reasonably well and allowed a large-scale evaluation of the inverted flow concept to be made. The static data were acquired at the Boeing test facility at Boardman, Oregon, while the simulated flight data were measured in the NASA-Ames Research Center 40×80 ft wind tunnel, hereafter referred to as 40×80 . The feasibility of using the 40×80 to determine flight effects on engine noise was established by NASA Ames contract NAS2-8213.^{2,4} The program included model tests with near- and far-field measurements and full-scale JT8D engine tests using near-field measurements. The model test showed that flight effects measured in the near field are the same as those measured in the far field. The JT8D engine test showed that the flight noise determined in the wind tunnel

matched measured flight noise of the 727/JT8D for a baseline and quiet nacelle installation. This paper summarizes the results of the JT8D inverted flow program that included the following major elements:

- 1) Design and fabrication of a primary/fan inverter duct for the JT8D engine.
- 2) A static, free field test to define far-field noise characteristics and establish near- to far-field correlations.
- 3) A flight effects test in the 40×80 .

Wind tunnel-derived flight effects for the JT8D with inverted flow and a conical nozzle are compared with corresponding results previously obtained for the JT8D configured as a baseline and internal mixer. Static and wind-tunnel tests were also conducted with Boeing-supplied nozzle variations to further explore the noise suppression potential of the inverted flow concept. The add-on configurations were designed to increase the mixing perimeter and mixing rate of the high-velocity primary flow. This was done by replacing the conical nozzle with a plug nozzle and a 20-lobe nozzle. The effect of an acoustic shield on noise was also evaluated.

Test Description

Static and wind-tunnel tests were conducted with a JT8D-17R turbofan engine. At sea level static conditions the engine has a bypass ratio of 1.1, a nominal airflow rate of 148 kg/s (326 lb/s), and develops a thrust of 77.9 kN (16,400 lb) at a pressure ratio of 2.2. An inverter duct was designed to divert the fan flow to an inner annulus and the primary flow to an outer annulus. The welded assembly includes eight fan and eight primary gas flow passages and has a length of 0.914 m (3 ft). Some mixing occurs between the two streams prior to exhausting through a conical nozzle. In addition to the conical nozzle, the inverter was tested with a conical plug nozzle and a 20-lobe nozzle. The latter nozzle was tested with and without an acoustically lined shield. A conventional JT8D baseline configuration was also tested to provide data for comparison with the inverter configurations. All noise tests were conducted with an acoustically treated two ring inlet in order to minimize inlet radiated fan noise. A schematic drawing of the test configurations is shown in Fig. 1.

The static test was conducted at a Boeing facility located at Boardman, Oregon (Fig. 2). The purpose of this test was to

Presented as Paper 79-0614 at the AIAA 5th Aeroacoustics Conference, Seattle, Wash., March 12-14, 1979; submitted March 30, 1979; revision received June 29, 1979. Copyright © American Institute of Aeronautics and Astronautics, Inc., 1979. All rights reserved. Reprints of this article may be ordered from AIAA Special Publications, 1290 Avenue of the Americas, New York, N.Y. 10019. Order by Article No. at top of page. Member price \$2.00 each, nonmember, \$3.00 each. Remittance must accompany order.

Index category: Noise.

*Noise Research Engineer, Noise Technology Staff.

†Research Engineer, U.S. Army Air Mobility Research and Development Laboratory.

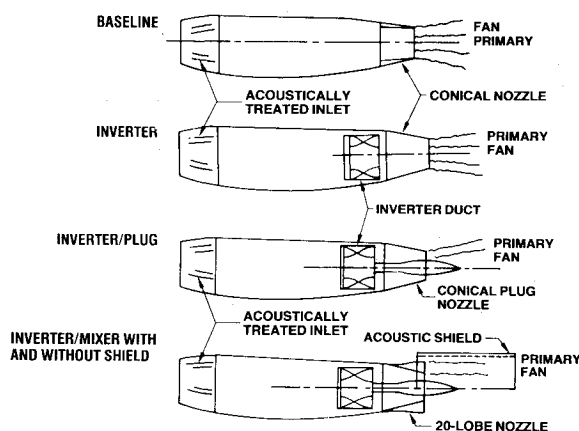


Fig. 1 Test configuration schematic.

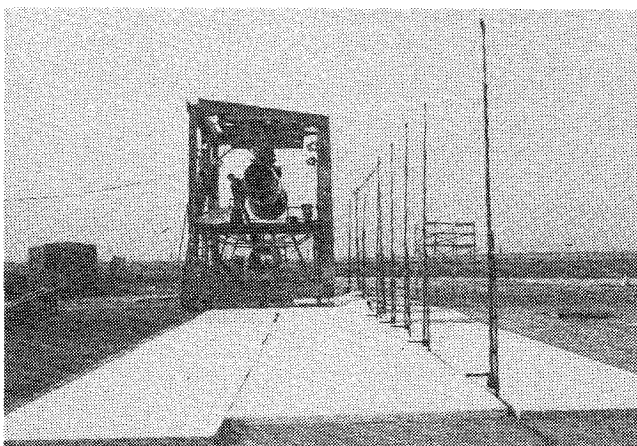


Fig. 2 JT8D installation at Boardman test site.

establish proper engine match, measure thrust performance, and define static far-field noise characteristics and near-to far-field correlations. The engine is mounted on a steel test stand at a height of 4 m (13 ft) above a concrete acoustic arena. Three microphone arrays were located on 3.05, 15.2, and 30.5 m (10, 50, and 100 ft) sidelines. The near array employed centerline height microphones that covered a range of angles from 30 to 165 deg referenced to the inlet axis and centered at the nozzle exit plane. Polyurethane foam was placed on the surface between the engine and centerline microphones to duplicate the wind-tunnel installation. The intermediate and far-field arrays used ground microphones that covered angles from 30 to 160 deg and 50 to 155 deg, respectively. Noise and performance data were measured for a wide range of engine power conditions from idle to pressure ratio 2.2. Corresponding primary jet velocities ranged from 140 to 590 m/s (460 to 1935 ft/s). The noise data were reduced in the form of 1/3 OB spectra.

The flight effects test was conducted in the NASA ARC 40 × 80 ft wind tunnel. A test installation photo is provided in Fig. 3 showing the side-mounted JT8D engine and the traversing microphone system. The view in Fig. 4 shows the 20-lobe nozzle with plug and lined acoustic shield. The lobes were designed to penetrate the outer primary flow and rapidly mix this flow with ambient air. The shield was designed to reflect and absorb the high-frequency premerged noise generated by the 20-lobe nozzle. About 400 m² of 7.6 cm thick polyurethane foam covered the test section floor and partly up the sidewalls. The engine was mounted at a height of 4 m above the floor. The two traverse microphones were located on a 3.05 m (10 ft) sideline at about engine centerline height. Noise data were recorded during a slow microphone sweep (0.15 m/s) that covered a range of angles from 30 to

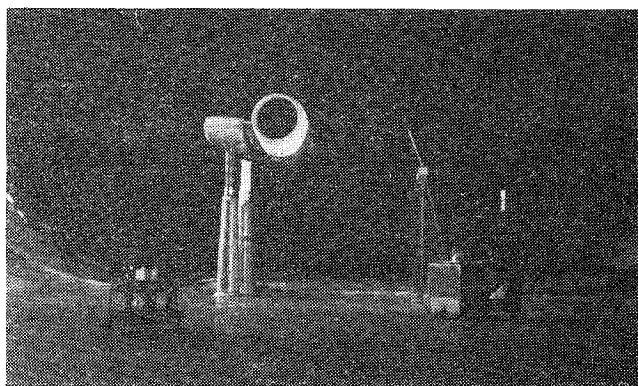


Fig. 3 Test installation in 40 × 80 wind tunnel.

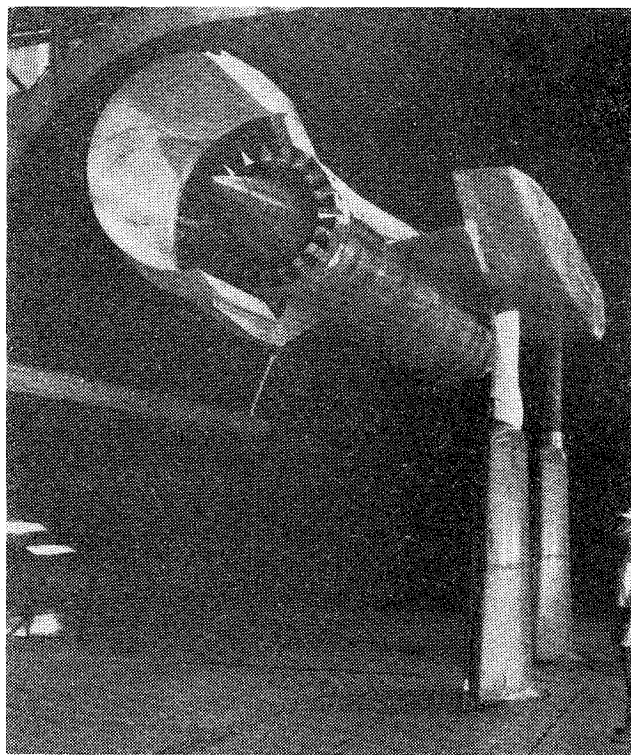


Fig. 4 Inverter/20-lobe mixer configuration with acoustic shield.

168 deg. The sweep data were reduced to define 1/3 OB spectra each 5 deg from 30 deg through 165 deg. A 1-s integration time was used, 0.5 s before and after the desired angle.

Wind-off and wind-on tests were run for the inverter configurations for a range of power conditions comparable to the static test. Tunnel velocities varied from a low of 55 m/s (180 ft/s) to a high of 95 m/s (310 ft/s). The wind-on engine noise data were corrected by logarithmically subtracting measured tunnel background noise. A reverberant field noise level was estimated by combined measurement and analysis techniques. Both wind-off and wind-on data were corrected for the reverberant field noise level in a manner similar to the background noise correction.

Data Analysis Technique

The noise measurements in the 40 × 80 wind tunnel were made relatively close to the engine noise sources. The sideline distance was selected as a compromise between the reverberant field, background noise, dominant near-field effects, and direct signal strength. The technique for determining flight effects in a closed wind tunnel requires that noise source locations and directivities be known for the frequencies of

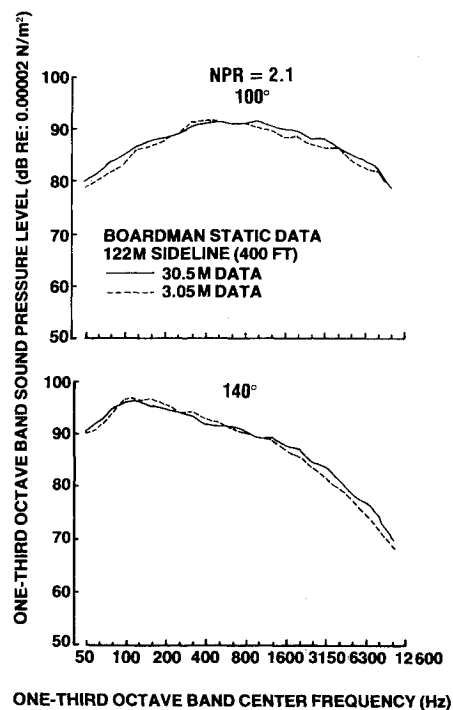


Fig. 5 Comparison of near- and far-field spectra, inverter.

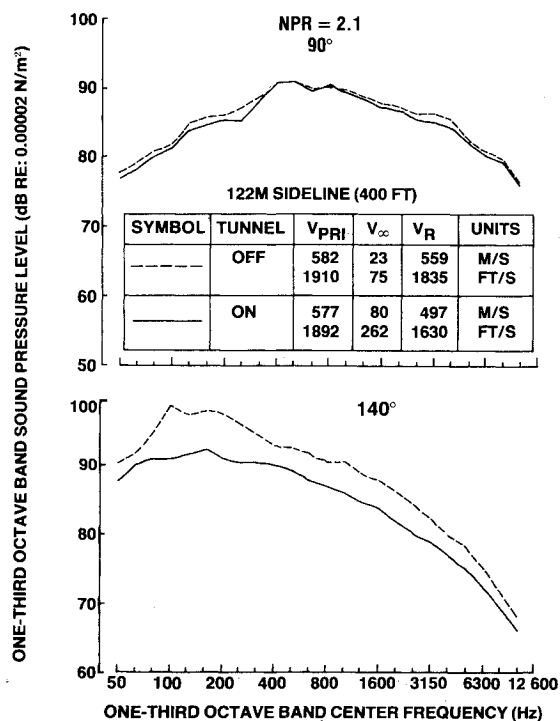


Fig. 7 Comparison of wind-off and wind-on spectra.

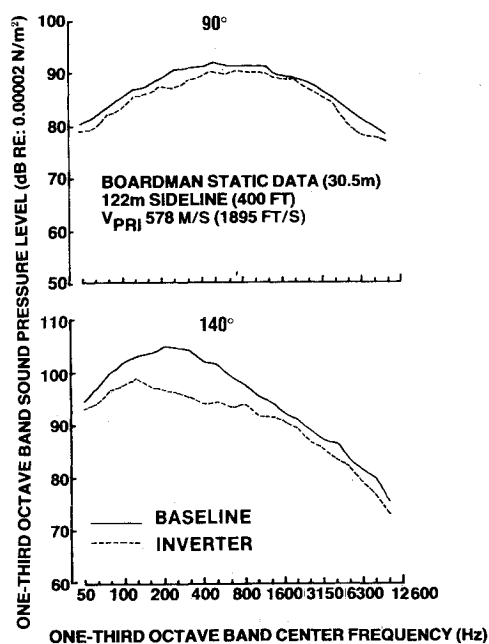


Fig. 6 Comparison of baseline and inverter spectra.

interest.^{2,4} The multiple sideline noise measurement procedure was used to define the required source location correlations as described in Ref. 4.

The correlations were verified by comparing data extrapolated from the three sidelines to a common far-field sideline. An example is provided in Fig. 5 where extrapolated 3.05 and 30.5 m spectra for the inverter configuration are compared. The good agreement is typical of results for a range of angles and power conditions.

The measured wind-tunnel data were corrected for background noise and reverberant field as previously mentioned. A computer program extrapolated the corrected data to the far field using the verified source location curves. Corrections were also made for convection as a function of propagation path length and tunnel velocity.

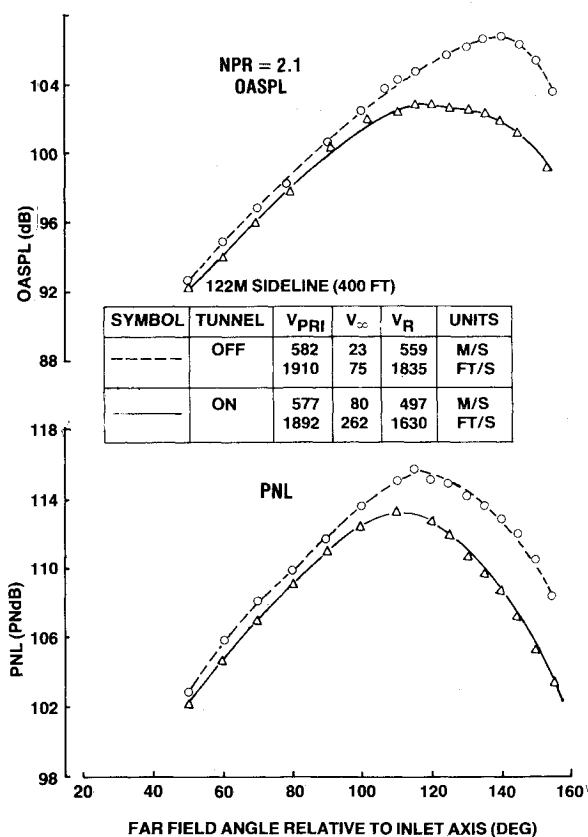


Fig. 8 Comparison of wind-off and wind-on OASPL and PNL directivities.

Basic Inverter Results

The static and wind-tunnel (flight) results for the basic inverter configuration are presented and discussed in this section. The basic inverter included the inverter duct and a conical exhaust nozzle. Results are compared with similar data for the JT8D engine configured as a baseline (uninverted

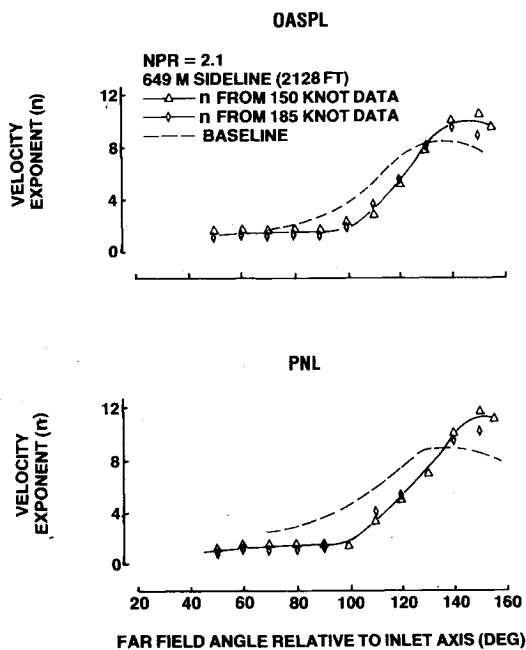


Fig. 9 Velocity exponents for OASPL and PNL, inverter.

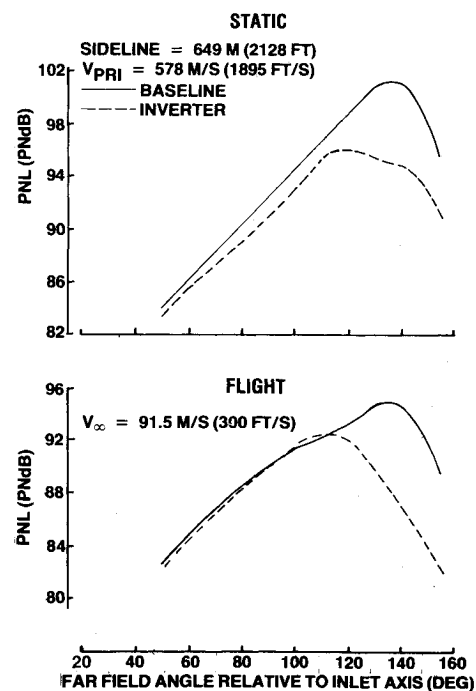


Fig. 11 Comparison of static and flight PNL directivity.

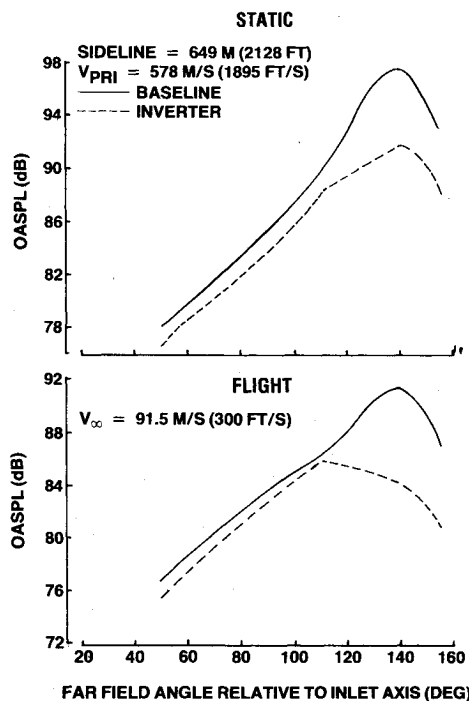


Fig. 10 Comparison of static and flight OASPL directivity.

flow) and an internal mixer (mixed flow). Wind-tunnel data for the latter two configurations were obtained during a previous test in the 40×80 .²

Baseline and inverter spectra from the static test are compared in Fig. 6 for takeoff power (30.5 m data). At low angles through 90 deg, the inverter provides little noise reduction relative to the baseline. As the angle increases toward the jet axis, the amount of reduction or suppression increases in the low to middle frequencies (Fig. 6). Inverter wind-off and wind-on spectra are compared in Fig. 7 for a high-power condition (extrapolated 3.05 m data). Tunnel velocity causes little or no reduction of noise at low angles through 90 deg but substantial reduction at angles near the jet axis. The reduction of OASPL and perceived noise level (PNL) with tunnel velocity is illustrated in Fig. 8. The results of Fig. 8 are

converted to a velocity exponent n , as shown in Fig. 9, where

$$n = \frac{PNL_{static} - PNL_{flight}}{10 \log V_{pri} / (V_{pri} - V_{\infty})}$$

Velocity exponent curves defined for the baseline are included for comparison with the inverter. The velocity exponents of the inverter are greater than the baseline at angles above 130 deg. This implies a gain in suppression when the operating condition changes from static to flight. The reverse is true at angles below 130 deg where the baseline exponents are larger.

Baseline and inverter OASPL and PNL directivities are compared in Figs. 10 and 11 for static and flight operation. The takeoff power comparisons reflect 30.5 m data that have been extrapolated to a 649 m (2128 ft) sideline, using source location correlations. The flight noise values were determined by applying the velocity exponents of Fig. 9 to the static OASPL and PNL values. The peak OASPL suppression for the flight case is slightly lower than the static case (5.5 vs 6 dB). Flight causes a decrease in suppression at low angles and an increase at angles of 140 deg and higher. Forward velocity reduces the peak PNL suppression from 5.5 to 2.5 PNdB. The large loss of peak PNL suppression for the inverter (120 deg) relative to the baseline (135 deg). Generally, the velocity exponent of a given configuration is smaller at 120 deg than at 135 deg (see Fig. 9). Thus, the baseline experiences a significantly larger reduction of peak PNL than the inverter with forward velocity. This result is fairly typical of suppressor nozzles, since most are dominated by high frequency noise and have peak PNL's in the 110 to 120 deg region. Baselines are usually dominated by low frequencies with peak PNL's in the 130 to 140 deg region. The low-frequency noise at high angles will be reduced more than the high-frequency noise at low angles and a loss of peak PNL suppression results. The in-flight PNL suppression at low angles (Fig. 11) is essentially zero. At angles of 140 deg and higher, the in-flight PNL suppression exceeds the static value. In summarizing the results of Figs. 10 and 11, the basic inverter provides effective in-flight suppression of OASPL at angles of 120 deg and higher and PNL at 125 deg and higher.

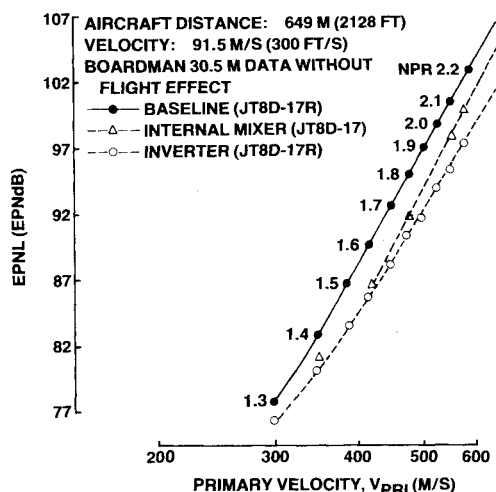


Fig. 12 Comparison of EPNL, static levels.

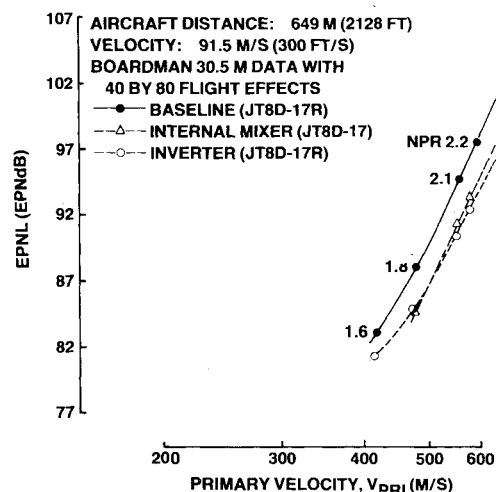


Fig. 13 Comparison of EPNL, flight levels.

The effective perceived noise level (EPNL) characteristics of the baseline, inverter, and internal mixer are compared in Figs. 12 and 13 as a function of primary jet velocity. For this study, EPNL is the logarithmic summation of PNL (rather than PNL_T). The calculation assumes a single engine moving past an observer at a velocity of 91.5 m/s (300 ft/s) and a distance of 649 m (2128 ft). Installation on an aircraft, angle of attack, flight trajectory, ground reflections, and extra ground attenuation are factors that are not included in the calculation.

The static EPNL's of Fig. 12 are calculated, assuming static PNL values that are unchanged by forward velocity. The flight EPNL's of Fig. 13 are based on the static EPNL's corrected to flight by means of velocity exponents similar to Fig. 9. At takeoff power (600 m/s) and with static PNL's, the inverter provides 5 EPNdB of suppression relative to 2 EPNdB for the internal mixer. Under flight conditions, the suppression values are 4 EPNdB for the inverter and 3 EPNdB for the internal mixer. Thus, the inverter loses 1 EPNdB and the internal mixer gains 1 EPNdB due to aircraft velocity. Although the inverter provides slightly more in-flight EPNL suppression, the margin is sufficiently less than indicated by static PNL data. It is noted that the internal mixer experiences less thrust loss than the inverter configured for this test. Thus, for equal thrust operation at power settings below full takeoff, the suppression advantage likely favors the internal mixer.

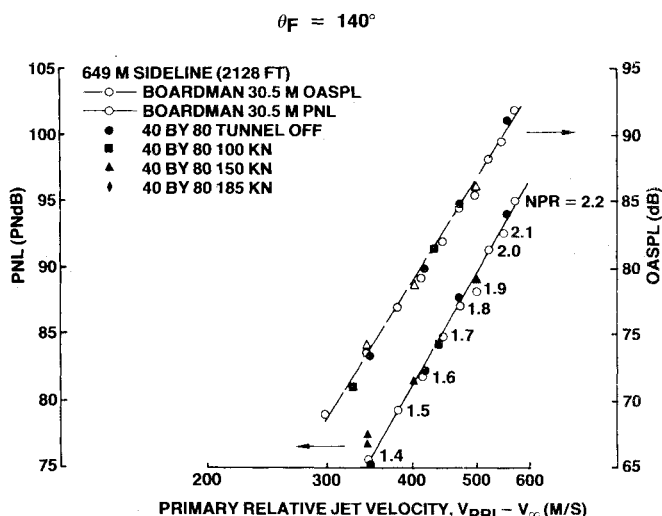


Fig. 14 Wind-off and wind-on OASPL and PNL vs primary relative velocity.

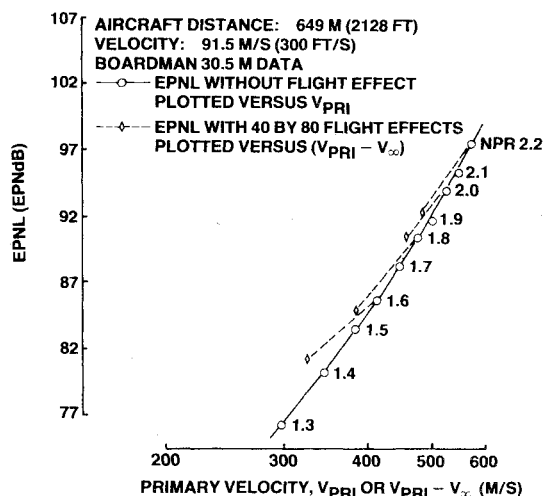


Fig. 15 Comparison of static and flight EPNL, inverter.

There is a trend, indicated in Fig. 13, that increasing the primary jet velocity beyond 600 m/s will favor the suppression potential of the inverted flow profile. Higher jet velocities will shift the peak PNL of the inverter to a higher angle where a more favorable flight effect will result. This is of importance to AST engines where primary jet velocities of about 760 m/s will be required during takeoff operations.

Another approach at evaluating flight effects on engine noise is to compare static and flight noise levels as a function of relative velocity. A typical example is provided in Fig. 14 for OASPL and PNL at an angle of 140 deg. At this angle, the flight OASPL and PNL values fall on the static data throttle line. Thus, the relative velocity principle can be applied for estimating flight OASPL and PNL from static data. At low angles, the flight noise levels are well above the throttle line. For the inverter configuration, the use of relative velocity will provide a good flight estimate of OASPL and PNL at angles of 120 deg and higher. At lower angles, the application of velocity exponent curves, such as Fig. 9, will define a more realistic flight noise level.

A somewhat similar type of comparison is shown in Fig. 15 where flight EPNL's are compared with equivalent static values. As indicated, the departure of flight EPNL's from the throttle line is significant and generally increases at reduced power. The same comparison for the baseline (Fig. 16) indicates that the flight EPNL's are slightly closer to the throttle line than the inverter.

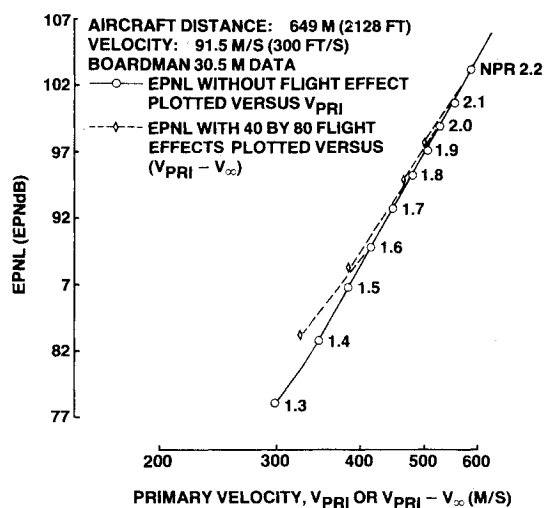


Fig. 16 Comparison of static and flight EPNL, baseline.

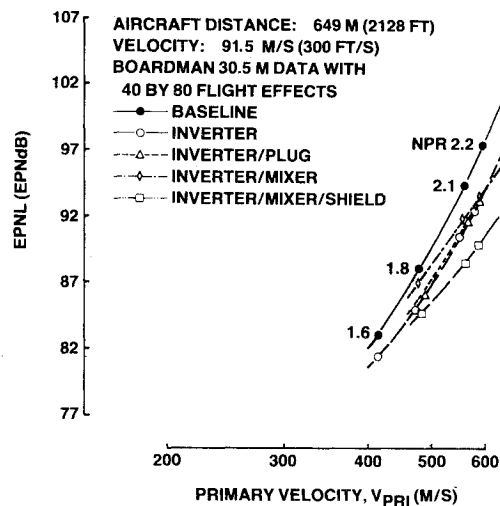


Fig. 18 Comparison of EPNL, flight levels.

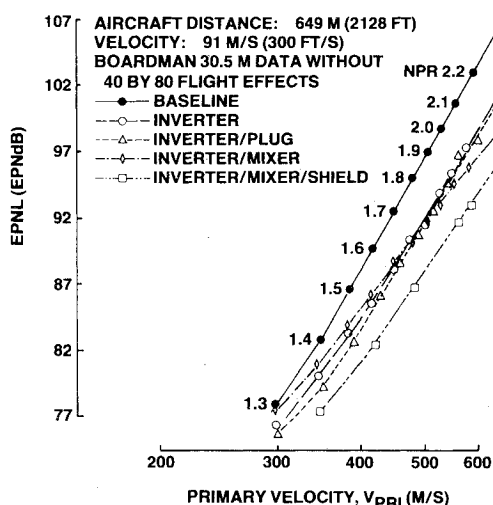


Fig. 17 Comparison of EPNL, static levels.

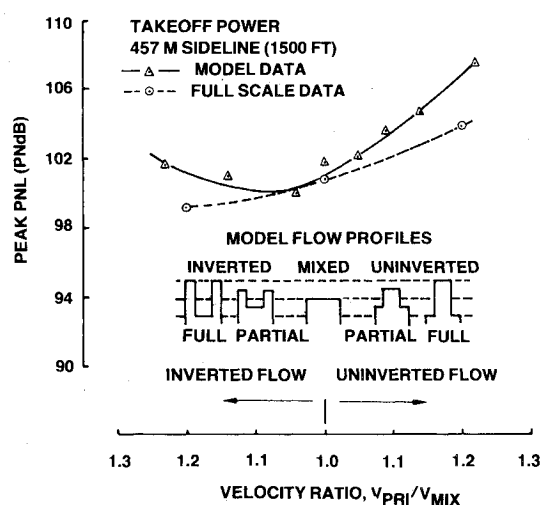


Fig. 19 Model and full-scale peak PNL vs velocity ratio.

Inverter with Nozzle Variations Results

The static and flight noise characteristics of the various inverter configurations are compared on the basis of EPNL results. EPNL values assuming no change in static PNL with flight are compared in Fig. 17. Configurations include the baseline, basic inverter, inverter with plug nozzle, inverter with 20-lobe nozzle, and inverter with 20-lobe nozzle and acoustic shield. At takeoff power (600 m/s), the inverter and inverter with plug both show about 5 EPNdB suppression. The 20-lobe nozzle has a suppression of 7 EPNdB without shield and 10 EPNdB with shield.

The in-flight EPNL characteristics are compared in Fig. 18. At takeoff power, the inverter, inverter with plug nozzle, and inverter with 20-lobe nozzle all provide a suppression of about 4 EPNdB. The largest suppression (7.5 EPNdB) is achieved by the 20-lobe nozzle with acoustic shield. The shield is effective in reducing aft-radiated, premerged mixing noise that is generated by the 20-lobe nozzle. This results in lower static PNL values and allows a larger reduction in PNL with flight for angles near the jet axis. The spectra, with minimum premerged mixing noise, is dominated by low-frequency postmerged mixing noise. The flight effect on this component is significantly larger than the flight effect on premerged mixing noise.

The 20-lobe nozzle without shield is reasonably effective in reducing PNL and EPNL under static conditions. Due to the strength of the premerged mixing noise components, the

reduction of PNL with forward velocity is relatively small at all angles. The EPNL suppression is 3 EPNdB less in flight than under static conditions for this configuration. The suppression potential of the 20-lobe nozzle will improve relative to the basic inverter as jet velocity is increased above 600 m/s. The premerged mixing noise component becomes less important in relation to the postmerged component. The result is a larger reduction of aft-quadrant PNL with forward velocity and improved in-flight PNL or EPNL suppression characteristics.

Engine thrust was measured during the static test. At takeoff power, the thrust losses in relation to the baseline are 1.5% for the basic inverter, 3% for the inverter/plug, and 5% for the 20-lobe nozzle configurations. Thrust performance, system weight, and complexity are important factors that must be evaluated in assessing the potential of a suppressor concept for a given application.

Model Results

Model tests were conducted at Boeing prior to the JT8D engine inverted flow program. The 1/7th scale models were tested under static conditions to determine the influence of flow profile on jet noise characteristics. Model and full-scale peak PNL values are plotted vs the velocity ratio in Fig. 19.

The model results show nearly equal PNLs for mixed and fully inverted flows and a minimum PNL at a partially inverted profile. For the partially inverted profile, the outer

Table 1 Summary of inverter suppression characteristics

Configuration	OASPL suppression, dB			PNL suppression, PNdB			EPNL suppression, EPNdB		
	Static	Flight	Change	Static	Flight	Change	Static	Flight	Change
Inverter	6.0	5.5	-0.5	5.5	2.5	-3.0	5.0	4.0	-1.0
Inverter/plug	5.0	6.0	+1.0	6.0	3.5	-2.5	5.2	4.0	-1.2
Inverter/20-lobe nozzle	9.5	5.0	-4.5	5.0	0.5	-4.5	7.0	4.0	-3.0
Inverter/20-lobe shield	10.5	7.0	-3.5	7.5	3.0	-4.5	9.8	7.5	-2.3
Internal mixer	2.0	3.0	+1.0	2.0	2.5	+0.5	2.0	3.0	+1.0

Note: Peak noise suppression relative to baseline at takeoff power and 649 m (2128 ft) sideline.

primary and inner fan velocities are between the fully mixed and fully inverted velocities. The engine results indicate that the inverted flow produces significantly lower peak PNL than the mixed flow. What appears to be a different finding may be the result of unique engine flow profiles created by the 12-lobe internal mixer and 16-element inverter. The engine profiles are not as well defined as the models; thus, the effective velocity ratios likely differ from those identified in Fig. 19. If both engine velocity ratios moved to the right, as is likely the case, then the engine curve would be more compatible with the model results. This analysis indicates that model flow profile tests can be used to identify meaningful trends. However, application of model results to engine noise studies must give appropriate consideration to specific exhaust profile variations expected for the engine.

Major Findings

The following findings are made as a result of the test program to determine static- and wind tunnel-derived flight noise characteristics of the JT8D-17R engine with inverted primary and fan flows. The suppression results described are relative to the baseline configuration (uninverted flow) and reflect takeoff power at a 649 m sideline. A summary of static and flight EPNL and peak OASPL and PNL suppression values is provided in Table 1.

1) The basic inverter configuration (inverter with conical nozzle) provides an in-flight EPNL suppression of 4.0 EPNdB. The comparable static suppression (summation of static PNL's) is 5.0 EPNdB, indicating a relatively modest loss of EPNL suppression due to flight.

2) The inverter with 20-lobe nozzle and lined acoustic shield provides the largest EPNL suppression of the configurations that were tested. A suppression potential of 10.0 EPNdB, based on static data, is reduced to 7.5 EPNdB by forward velocity. The shield is effective in minimizing premerged mixing noise at angles near the jet axis.

3) Forward velocity causes a significant loss of peak PNL suppression. For the basic inverter, the peak PNL suppression is reduced from a static value of 5.5 PNdB to a flight value of 2.5 PNdB. The inverter configurations are effective in reducing PNL at angles of 125 deg and higher, but ineffective at lower angles where peak noise occurs.

4) Forward velocity results in a small loss in peak OASPL suppression for the inverter. The in-flight suppression is 5.5 dB relative to a static value of 6.0 dB. A slight gain in suppression occurs for the inverter with plug nozzle, while a more significant loss of suppression is experienced by the 20-lobe nozzle configurations. In general, significant in-flight OASPL suppression is achieved at angles of 120 deg and higher.

5) The inverted flow provides lower EPNL than the mixed flow for static conditions and comparable EPNL under flight conditions. Static suppression values are 5.0 EPNdB for the basic inverter and 2.0 EPNdB for the internal mixer. In-flight suppression values are 4.0 and 3.0 EPNdB, respectively. Forward velocity causes a slight loss of suppression for the inverter and a slight gain for the mixer. This significantly narrows the noise suppression advantage of the inverted flow profile for flight operation.

6) Thrust loss is experienced by the inverter configurations. Relative to the baseline performance, the loss ranges from 1.5% for the basic inverter to 5.0% for the 20-lobe configurations. Thrust performance, system weight, and complexity are important factors that will impact the effectiveness of these concepts for application on a particular aircraft.

7) Static model flow profile noise studies indicate some differences when compared with full-scale results. Part of the differences are thought to be caused by unique, nonuniform engine flow profiles created by the 12-lobe internal mixer and multiduct inverter configurations. By contrast, the model profiles were well-defined regions of primary and fan flow.

References

- ¹Strout, F.G., "Flight Effects on Noise Generated by the JT8D Engine with Inverted Primary/Fan Flow as Measured in the NASA-Ames 40- by 80-Foot Wind Tunnel," NASA CR-2996, June 1978.
- ²Strout, F.G., "Flight Effects on Noise Generated by the JT8D-17 Engine in a Quiet Nacelle and a Conventional Nacelle as Measured in the NASA-Ames 40- by 80-Foot Wind Tunnel," NASA CR-137797, Jan. 1976.
- ³Strout, F.G., "Flight Effects on Noise Generated by the JT8D-17 Engine in a Quiet Nacelle and a Conventional Nacelle as Measured in the NASA-Ames 40- by 80-Foot Wind Tunnel—Summary Report," NASA CR-2576, June 1976.
- ⁴Jaek, C.L., "Static and Wind Tunnel Near Field/Far Field Jet Noise Measurements from Model Scale Single-Flow Baseline and Suppressor Nozzles—Summary Report," NASA CR-2841, June 1977.